ISSN 1392-1207. MECHANIKA. Vol. 30, No. 3, 2024: 228–235

Finite Element Analysis of Laser Ablation Damage and Buckling Mode of Axially Compressed CFRP Cylindrical Shell

Guang YANG, Xiaodong XING, Weilong GUO, Liquan WANG
College of Mechanical and Electrical Engineering, Harbin Engineering University, Harbin 150001, China,
E-mails: sun5sun5sun@163.com, xingxiaodong@hrbeu.edu.cn (Corresponding author), guoweilong@hrbeu.edu.cn, wangliquan@hrbeu.edu.cn
https://doi.org/10.5755/j02.mech.35807

1. Introduction

Carbon fiber reinforced epoxy resin has become an advanced aerospace material due to its excellent thermodynamic properties and is used to manufacture structural components such as rockets and spacecraft shells [1]. During high-speed flight, in addition to enduring huge inertial overloads, aircraft may also be threatened by high-intensity directed energy radiation such as laser beams [2]. Carbon fiber reinforced composite materials (CFRP) will undergo complex physical and chemical processes in high-temperature environments, causing significant changes in material properties [3-4]. In particular, the ablation effect caused by laser heating reduces the load-bearing capacity of structural parts due to the degradation of material mechanical properties and material loss at high temperatures [5]. Thermal ablation effect is the most important damage method of laser weapons to aircraft [6]. The effect and damage mechanism of laser on composite materials have received widespread attention from researchers [7], including modeling, numerical simulation, and experimental research on the ablation process, mechanism, and its impact on structural strength.

The main research work on the ablation process and mechanism of composite materials is as follows. Dimitrienko et al. [8] studied the mesoscopic model of resin thermodynamic properties changing with the three-phase volume ratio and established functional relationships to describe the degree of pyrolysis of epoxy resin. Lachaud et al. [9] set up a modeling strategy to simulate the physical and chemical process of laser ablation of composite materials from microscopic scale (fiber, matrix), mesoscopic scale (bundle, matrix) and macroscopic scale (composite). Jinfeng Zhang [10] established a three-dimensional finite element model for simulating thermal ablation of laser irradiated composite materials based on the unit birth and death method, and studied the laser ablation effect of carbon fiber/epoxy resin composite laminates, including the temperature field and surface materials melting, disappearance and deformation process, as well as ablation morphology. The influence of laser and material thermodynamic parameters on laser ablation was analyzed as well. Weina Zhao et al. [11] established a multi-scale analysis model for the material thermal damage effect when continuous laser irradiation of CFRP laminates. The model was used to simulate the ablation, pyrolysis and interlayer cracking behaviors caused by high-power continuous laser, and the simulation results were in good agreement with the experimental results.

The research work on effect of laser ablation on the strength of composite materials and its damage mechanism is as follows. Kai Zhu et al. [12] used numerical simulation methods to obtain the constitutive relationship of the laser irradiated composite laminate model. Guoliang Peng et al. [13] proposed a model for calculating the energy coupling rate during laser ablation of glass fiber/epoxy resin composite materials. Dongsheng Fu et al. [14] used experimental methods to study the changes in parameters such as back surface temperature of T-700 carbon fiber/epoxy resin laminate structure after laser irradiation. Qian Li et al. [15] established a heating model describing the microstructure of fiber composite materials after being irradiated by laser, and simulated the thermal coupling behavior and real-time ablation morphology of composite material cells under laser irradiation. Hong Wan et al. [16] studied the damage modes and changes in the structure and mechanical properties of carbon fiber and high silica fiber reinforced epoxy resin and phenolic resin-based composites under continuous laser irradiation with different power densities. Liujie Xiong et al. [17] conducted an analysis of the strength of CFRP laminates under the combined action of laser and mechanical load, and predicted the influence of laser intensity and irradiation time on the tensile strength of the laminates. Yongchao Han et al. [18] predicted the failure time of carbon fiber/epoxy resin reinforced composite (CFRC) laminates, and experimentally studied the failure mechanism under different factors such as laser power density, prestress level, and spot size. The influence rules of these factors on fracture time were obtained.

Since laser ablation damage of CFRP materials is a very complex process, there is still a lack of in-depth research on the impact of ablation damage on the structural load-bearing capacity, as well as the effects of different factors such as laser parameters and irradiation position. We use ALE adaptive mesh technology to simulate the dynamic ablation and buckling failure process of laser irradiation CFRP axial compression cylindrical shell structure through finite element simulation method, and analyze the influence of laser irradiation position on the buckling failure of axial compression cylindrical shell.

2. Numerical model of laser ablated CFRP cylindrical shell under axial compression

2.1. Laser irradiation heat conduction

The cylindrical shell material is T300 /914 carbon fiber epoxy composite. This material has good heat resistance and low thermal conductivity. When the temperature exceeds 300 degrees Celsius, thermal decomposition begins. When the temperature is higher than 600 degrees Celsius, the pyrolysis is completed [19]. The heat transfer

process involving ablation is described by the heat conduction equation [19]:

$$\rho c\frac{\partial T}{\partial t}=\frac{\partial}{\partial x_i}\left(\lambda_{ij}\frac{\partial T}{\partial x_j}\right)\delta_{ij}-T\beta^{ij}\dot{\gamma}_{ij}+\dot{Q}_{laser}+\dot{Q}, \quad (1)$$

where $T(x, y, z, t)$ represents the temperature field of the structure at time t; ρ, c and λ represent the density, specific heat and thermal conductivity respectively, and λ has three independent parameters, which are λ_{ij}. $T\beta^{ij}\dot{\gamma}_{ij}$ represents the heat caused by deformation work, β^{ij} is the material physical property coefficient, $\dot{\gamma}_{ij}$ is called the coupling term; $\dot{Q}_{laser}$ is the laser heat source term; $\dot{Q}$ represents other heat source terms.

Thermal decomposition will form voids inside the material, and the energy dissipation caused can be represented by $\dot{Q}$. The thermal decomposition energy dissipation here includes two parts: the heat absorption of the thermal decomposition reaction and the flow of pyrolysis gas flow. The total energy dissipation can be expressed as:

$$\dot{Q}=Q_{deco}\frac{\partial\rho}{\partial t}-\left(\phi_g\rho_g\bar{v}_g\right)\nabla h_g, \quad (2)$$

$$\frac{\partial\rho}{\partial t}=-\nabla\left(\phi_g\rho_g\bar{v}_g\right), \quad (3)$$

where Q_{deco} represents the heat of thermal decomposition of the material, ρ represents the density of the material, φ_g, ρ_g, $\bar{v}_g$, h_g respectively represents the volume fraction, density, flow rate vector and enthalpy of the pyrolysis gas.

The oxidation reaction of carbon fiber will cause surface ablation, and the energy dissipation caused at the boundary is related to the oxidation rate. The oxidation rate is controlled by two processes, the surface oxidation and the transport of external oxygen to the surface [19].

The laser irradiation boundary is shown in Fig. 1, where q_{laser} represents the laser heat flow absorbed by the surface, q_{cond} represents the heat flow from the boundary to the interior of the structure, and q_{abl} represents the heat flow taken away by material ablation at the boundary.

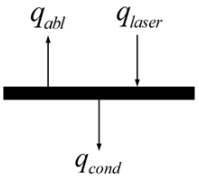

Fig. 1 Laser irradiation boundary conditions

The boundary conditions of the laser irradiation surface are:

$$q_{laser}=q_{cond}+q_{abl}. \quad (4)$$

The laser heat flow absorbed at the boundary can be expressed as:

$$q_{laser}=A(T)I_0(x,y,z;t), \quad (5)$$

where $A(T)$ is the laser surface absorptivity and $I_0(x, y, z; t)$ is the incident laser energy distribution.

The heat flow from the boundary to the interior of the structure can be expressed by Fourier's law as:

$$q_{cond}=\lambda_{nn}\frac{\partial T}{\partial n}, \quad (6)$$

where n represents the normal outward unit vector on the boundary, and λ_{nn} represents the normal thermal conductivity coefficient.

The heat taken away by material ablation at the boundary is related to the surface ablation rate and is expressed by the following formula:

$$q_{abl}=\dot{m}Q_{abl}, \quad (7)$$

where $\dot{m}$ is the mass flow rate caused by ablation, and q_{abl} is the ablation heat.

Table 1

Thermal property parameters of T300/914 carbon fibre epoxy composite

Temperature, K	λ_{11}, W/(m·K)	λ_{22}, W/(m·K)	λ_{33}, W/(m·K)	C, J/(Kg·K)	ρ, kg/m^3
311	0.033	0.033	0.35	1027.778	1458
350	0.034	0.034	0.37	1027.778	1458
400	0.037	0.037	0.39	1027.778	1458
561	0.044	0.044	0.47	1027.176	1455.95
634	0.049	0.049	0.55	1018.824	1428.21
700	0.056	0.056	0.80	981.7158	1316.74
748	0.058	0.058	1.05	938.7894	1208.03

Table 2

Mechanical properties of T300/914 carbon fibre epoxy composite

Temperature, K	E_1, Pa	E_2, Pa	E_3, Pa	μ_{12}	μ_{13}	μ_{23}	G_{12}, P)	G_{13}, Pa	G_{23}, Pa
311	1.87×10^9	1.79×10^9	1.79×10^9	0.3	0.31	0.31	$4.72\times10_8$	4.72×10^8	4.72×10^8
350	4.17×10^8	3.85×10^8	3.85×10^8	0.3	0.31	0.31	$1.27\times10_8$	1.27×10^8	1.27×10^8
400	3.90×10^8	3.61×10^8	3.61×10^8	0.3	0.31	0.31	$1.20\times10_8$	1.20×10^8	1.20×10^8
561	3.01×10^8	2.78×10^8	2.78×10^8	0.3	0.31	0.31	$9.40\times10_7$	9.40×10^7	9.40×10^7
634	2.59×10^8	2.39×10^8	2.39×10^8	0.3	0.31	0.31	$8.16\times10_7$	8.16×10^7	8.16×10^7
700	2.22×10^8	2.05×10^8	2.05×10^8	0.3	0.31	0.31	$7.08\times10_7$	7.08×10^7	7.08×10^7
748	1.97×10^8	1.82×10^8	1.82×10^8	0.3	0.31	0.31	$6.33\times10_7$	6.33×10^7	6.33×10^7
870	1.45×10^8	1.34×10^8	1.34×10^8	0.3	0.31	0.31	$4.68\times10_7$	4.68×10^7	4.68×10^7

The thermal and mechanical performance parameters of the material T300/914 carbon fiber epoxy/resin composite were given in Table 1 and Table 2 [20].

2.2. Finite element model

The buckling failure process of cylindrical shells under laser ablation under axial compression is a thermal-mechanical coupling problem, involving heat conduction, thermal stress, ablation damage, buckling failure, geometric nonlinearity, material nonlinearity and boundary nonlinearity. The material parameters that change with temperature are obtained through thermogravimetric analysis (TGA), and geometric nonlinearity is introduced through eigenmode simulation. The ALE adaptive grid technology is used to simulate the surface ablation and decay process, and the Arrhenius equation [21] is used to fit the ablation changes:

$$K=Aexp(-E_a/RT), \tag{8}$$

where K is rate constant, A is pre-exponential factor, R is molar gas constant, E_a is apparent activation energy.

This is an empirical formula that expresses the relationship between the material's chemical reaction rate constant with temperature. Surface ablation and decay are based on experimental results, averaging the ablation mass loss onto the surface. The ablation surface recession criterion is set by writing the UMESHMOTION subroutine. The program flow chart is shown in Fig. 2 below.

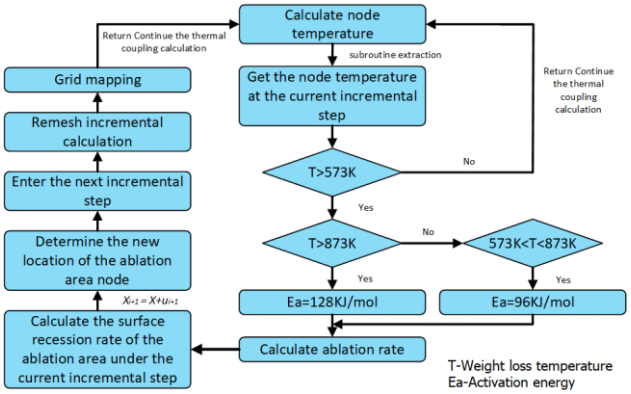

Fig. 2 Ablation model calculation flow chart

The length of the cylindrical shell model is L =1 m, the diameter is D = 0.4 m, and the shell thickness t = 0.02 m. The values of material thermal performance parameters are given in Table 1 and Table 2. The stacking sequences of the simulation model is $[90/45/-45/0]_{2s}$. We use the commercial software ABAQUS to establish a finite element model, adopt the thermal coupling analysis method, and select the C3D8T thermal displacement coupling unit with an 8-node unit. The number of grids is 13000. One end of the cylindrical model is fixed, and a compressive load of 0.001 m along the axial direction is applied to the other end. The time step is 0.001 s.

The damaging effect of laser ablation on axially compressed cylindrical shells is mainly reflected in the sharp increase in temperature in the irradiation area, resulting in changes in thermodynamic properties, and the material loss during the ablation process leads to a significant reduction in the load-bearing capacity of the cylindrical

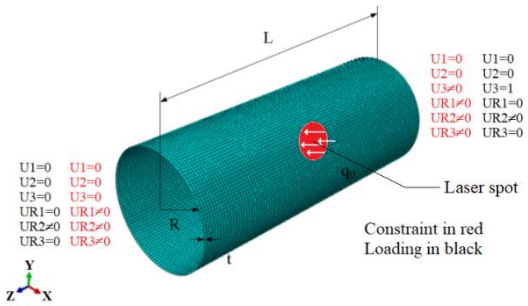

Fig. 3 Finite element model of laser irradiated axial compression cylindrical shell

shell [19]. The ablation of CFRP's resin matrix and carbon fiber in a high-temperature environment is a complex physical and chemical process. Thermal decomposition, sublimation phase change, and oxidation are the three main thermal ablation mechanisms of CFRP at high temperatures [22]. The complex ablation problem is simplified in this paper, a new constitutive relationship in the ablation region is given, and the impact of ablation on the critical buckling load (CBL) is investigated. The calculation process is as follows: through secondary development of ABAQUS, writing the Umeshmotion subroutine to control surface decay and the Dflux subroutine to control loading heat flow, first calculate the temperature field of the laser irradiated cylindrical shell, and extract the node temperature to determine the ablation area, and then conduct thermoelastic analysis. The specific calculation flow chart is shown in Fig. 4.

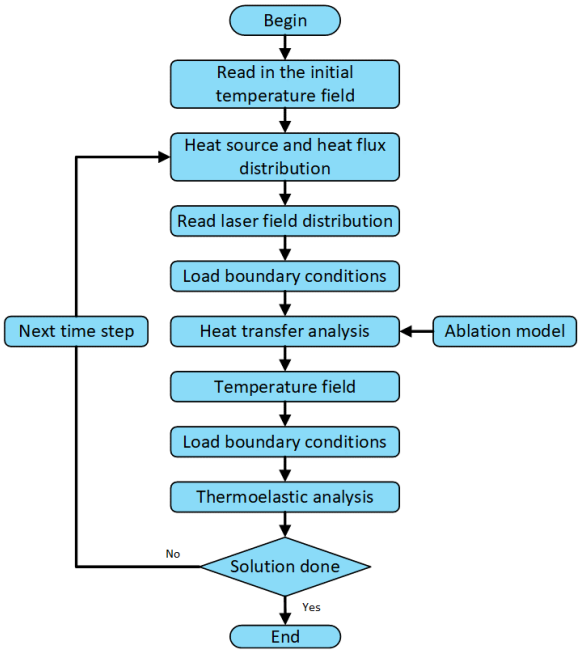

Fig. 4 Thermal-mechanical coupled analysis process considering ablation

3. T300/914 laminate ablation simulation analysis and verification

The flat plate ablation experiment was carried out to verify the feasibility of ABAQUS ALE adaptive grid technology to simulate ablation. The experiment set-ups are shown in Fig. 5. The American IPG Photonics YLS-2000 high-power laser was used to conduct ablation experiments

on irradiated flat plates in a laboratory environment, and experimental data such as ablation rate, ablation depth, and temperature rise curves were obtained. Two 50×50×5 mm T300/914 laminates, whose stacking sequences is $[90/45/-45/0]_{2s}$, were irradiated with lasers with energy densities of 1273 W/cm2 and 2547 W respectively under ordinary air flow for 4 seconds, and the measured ablation depths were 21.9 μm and 1340.5 μm respectively. As mentioned in Section 2.2, applying the same modeling method and material

a

b

Fig. 5 Experiment set-ups: a – YLS-2000 optical fiber laser, b –T300/914 laminate

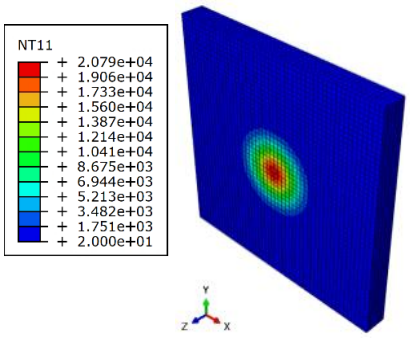

a

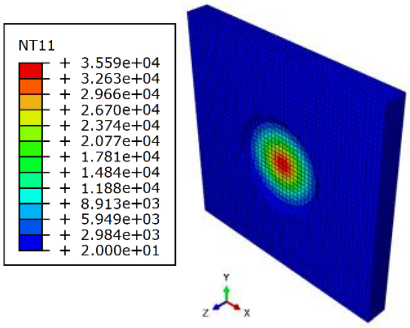

b

Fig. 6 Temperature field of laser irradiated test samples at *t*=4 s: a–1273 w, b –2547 w

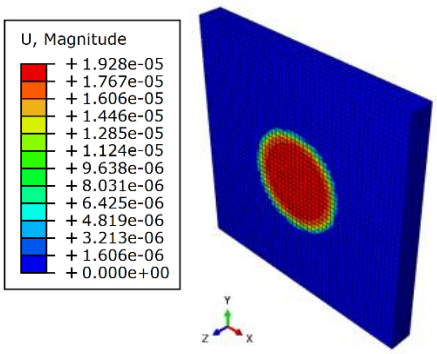

a

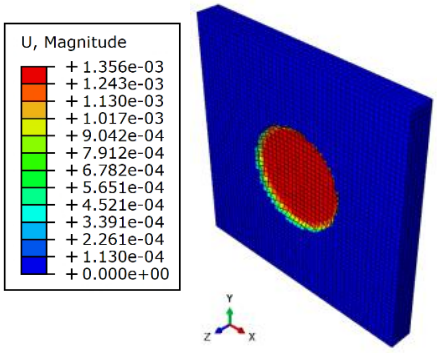

b

Fig. 7 Displacement field of laser irradiated test samples at *t*=4 s: a –1273 w, b –2547 w

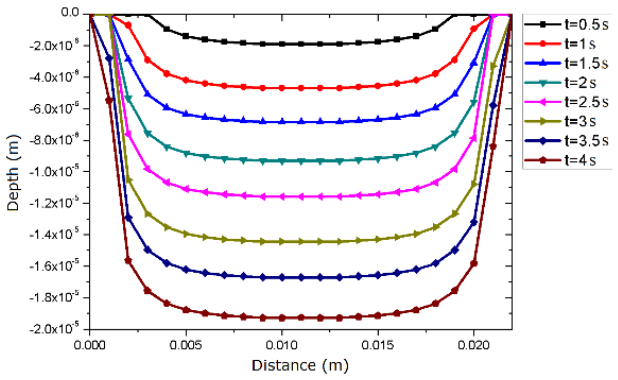

a

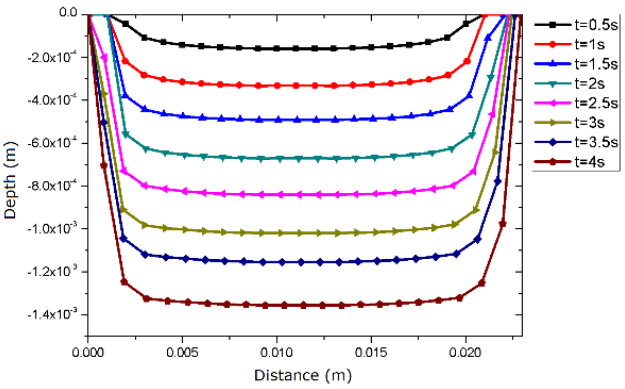

b

Fig. 8 Simulated real-time ablation displacement curve of the laser irradiated samples: a – 1273 w, b – 2547 w

properties, a finite element model of the flat plate under experimental conditions was established. The coupled temp-displacement module of ABAQUS and ALE adaptive mesh were used to simulate the ablation process of T300/914 laminates. The temperature field is obtained as shown in Fig. 6, and the displacement field is shown in Fig. 7.

The displacement curve at each moment is shown in Fig. 8. It can be seen that the simulation results are in good agreement with the experimental results, which verifies the feasibility of using ALE adaptive grid technology to simulate the ablation of T300/914 material through the ABAQUS subroutine UMESHMOTION.

4. Simulation analysis of buckling failure of laser ablation axial compression cylindrical shell

4.1. The influence of ablation on buckling failure of cylindrical shells

The changes in mechanical parameters after laser irradiation and the decrease in mechanical properties caused by material loss due to ablation are important factors affecting the CBL. At the same time, the effects of material nonlinearity, geometric nonlinearity and boundary nonlinearity should be considered. The buckling failure dynamic process of laser ablation axial compression CFRP cylindrical shell with a stacking sequence of $[90/45/-45/0]_{2s}$ is simulated by the finite element software ABAQUS. First, the finite element simulation method is used to predict the transient temperature field of the cylindrical shell under laser irradiation. Then extract the temperature values of the model nodes at the center of the laser spot at different time steps to obtain the temperature change curve of the spot center with time, as shown in Fig. 9. The buckling mode with and without ablation is shown in Fig. 10, the corresponding local enlarged view is shown in Fig. 11, and the cylinder end compressive displacement-load curve is shown in Fig. 11.

The resin matrix will thermally decompose at high temperatures. Carbon fiber has good thermal stability, but when the temperature rises to a certain level, carbon fiber will undergo sublimation phase change. These complex physical and chemical processes cause weight loss in the CFRP material. It can be seen from Figs. 10, 11 and 12 that laser irradiation causes ablation of the CFRP cylindrical shell, resulting in a decrease in the CBL and a change in the buckling mode.

4.2. The influence of laser ablation position

In order to analyze the effect of the laser irradiation

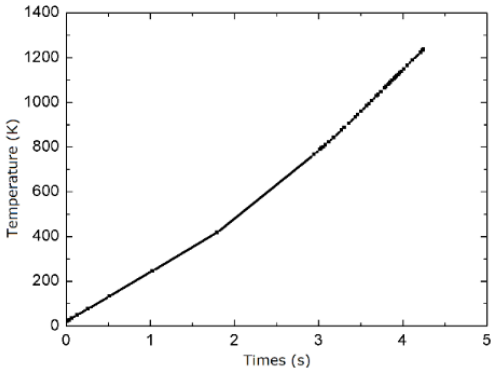

Fig. 9 Temperature rise curve at the center of laser spot

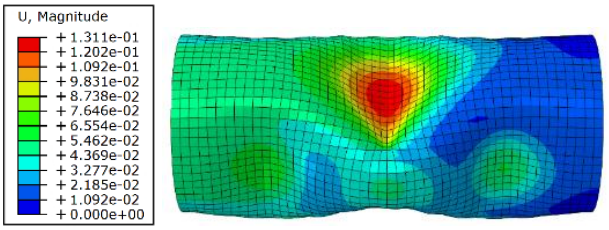

a

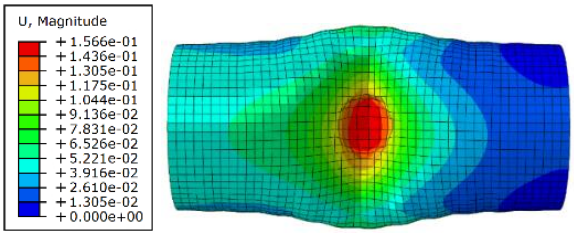

b

Fig. 10 Buckling modes of cylindrical shell structures: a – ignoring the ablation effect, b – considering ablation effect

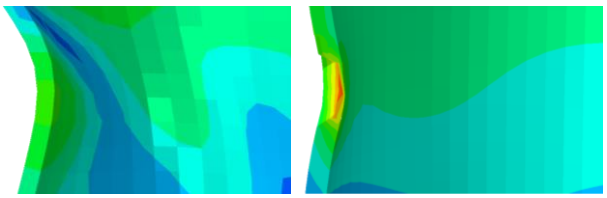

a b

Fig. 11 Local enlarged view of the cylindrical shell section at the laser irradiated position: a – heat softening, b – consider ablation effect

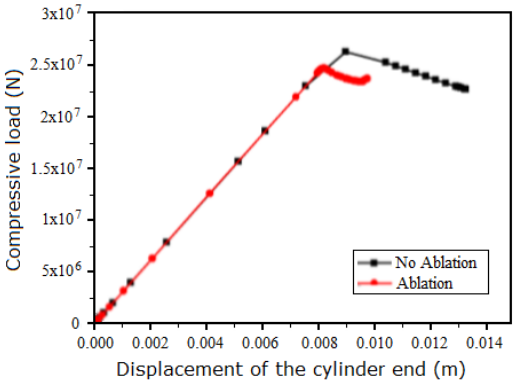

Fig. 12 The compressive load varied with the displacement

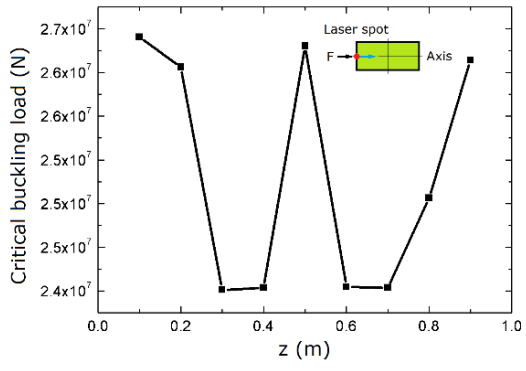

Fig. 13 The CBL varied with the laser spot positions

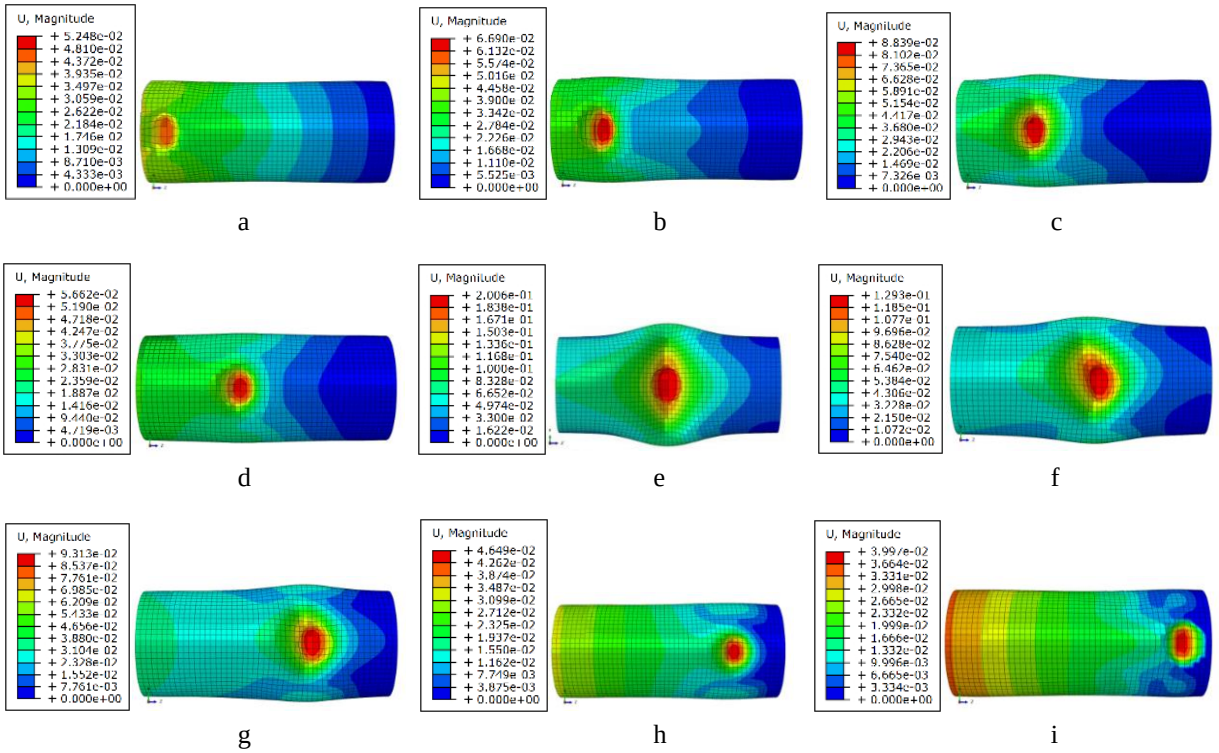

Fig. 14 Buckling mode when the spot moves along the axis: a – z = 0.1 m, b – z = 0.2 m, c – z = 0.3 m, d – z = 0.4 m, e – z = 0.5 m, f – z = 0.6 m, g – z = 0.7 m, h – z = 0.8 m, i – z = 0.9 m

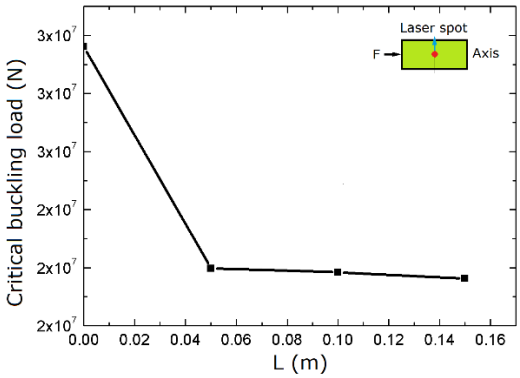

Fig. 15 The CBL varied with the deviating distance of the laser spot

position on the CBL, the laser spot moves along the axis of the cylindrical shell, taking z=0.1 m, 0.2 m, 0.3 m, 0.4 m, 0.5 m, 0.6 m, 0.7 m, 0.8 m, 0.9 m. The relationship between the spot position and the CBL is obtained as shown in Fig. 13, and the buckling modes are shown in Fig. 14.

The changing trend of the CBL is symmetrical about the cross-section passing through the midpoint of the cylindrical shell axis. When the laser spot moves from the loading end to the midpoint along the cylindrical shell axis, the CBL of the experimental model first decreases and then increases. It can be seen that when the laser irradiation position is between the end of the cylindrical shell and the midpoint of the axis, buckling failure of the axially compressed cylindrical shell is most likely to occur.

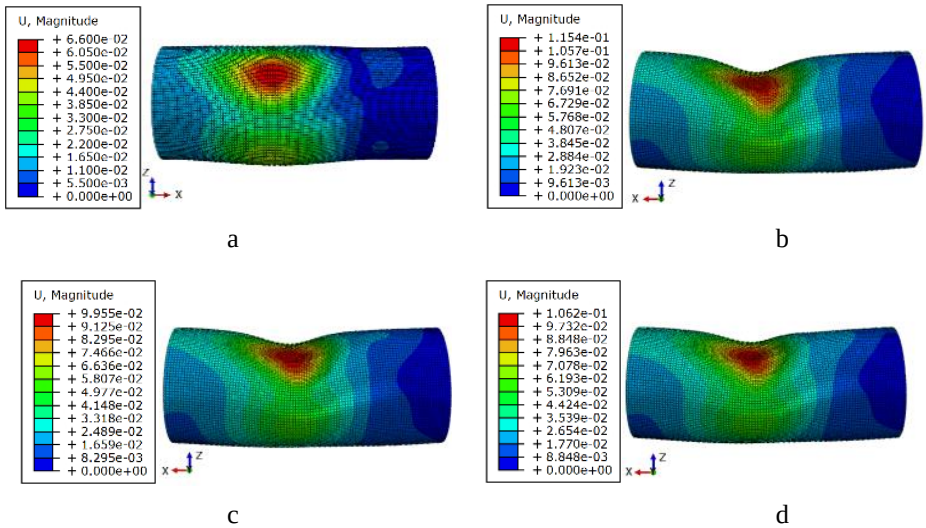

Fig. 16 Buckling modes at different spot positions: a – a = 0 m, b – a = 0.05 m, c – a = 0.1 m, d – a = 0.15 m

When the laser moves in the radial direction from the center of the cylindrical shell, take the offset distance a = 0 m, 0.05 m, 0.1 m, 0.15 m, and obtain the CBL under different offset distances, as shown in Fig. 15, and the corresponding buckling mode as shown in Fig. 16.

It can be seen from Figs. 15 and 16 that the CBL gradually decreases as the laser spot deviates from the axis in the radial direction. The load decreases sharply when it starts to deviate, and then tends to be gentle.

5. Conclusions

The buckling failure process of CFRP cylindrical shell under axial compression and laser ablation was studied through finite element simulation, and the influence of ablation itself and laser irradiation position on the CBL of the structure was discussed.

1. Through the secondary development of ABAQUS, the UMESHMOTION and DFLUX subroutines are called and combined with the ALE adaptive grid technology to simulate the laser ablation process of the T300/914 laminates. Compared with the ablation experimental results, the feasibility of ALE adaptive grid technology in simulating ablation of T300/914 material is verified.

2. Use ALE adaptive grid technology to simulate the ablation process of laser irradiation axial compression CFRP cylindrical shell. Ablation will significantly reduce the CBL of the structure.

3. For a cylindrical shell structure that is subjected to axial pressure or inertial load, taking the ablation effect into consideration, the laser spot position is between the end and the midpoint of the axis in the axial direction, and at the position farthest from the axis in the radial direction, the structure is most susceptible to buckling failure.

References

1. **Trellu, A.; Pichon, G.; Bouvet, C.; Rivallant, S.; Castanié, B.; Serra, J.; Ratsifandrihana, L.** 2020. Combined loadings after medium velocity impact on large CFRP laminate plates: Tests and enhanced computation/testing dialogue, Composites Science and Technology 196: 108194. https://doi.org/10.1016/j.compscitech.2020.108194.
2. **Kalisky, Y.; Kalisky, O.** 2011. Applications and performance of high power lasers in the battle field, Optical Materials 34(2): 457-460. https://doi.org/10.1016/j.optmat.2011.04.005.
3. **Dimitrienko, Y. I.** 1997. Thermomechanical behaviour of composite materials and structures under high temperatures: 1. Materials, Composites Part A: Applied Science and Manufacturing 28(5): 453-461. https://doi.org/10.1016/S1359-835X(96)00144-3.
4. **Dimitrienko, Y. I.** 1997. Thermomechanical behaviour of composite materials and structures under high temperatures: 2. Structures, Composites Part A: Applied Science and Manufacturing 28(5): 463-471. https://doi.org/10.1016/S1359-835X(96)00145-5.
5. **Chen, M.; Long, L. C.; Liu, S. B.** 2010. Destruction of composite material under tensile pre-stressing and laser irradiation, Chinese Journal of Applied Mechanics 27(2): 412-417 (in Chinese).
6. **Shi, W. B.; Li, S. X.; Xiao, Y.; Liu, S.** 2010. Laser Lethality of Hypersonic Vehicles under Aero-heating, High Power Laser and Particle Beams 22(6): 1215-1218 (in Chinese). https://doi.org/10.3788/HPLPB20102206.1215.
7. **Song, H. W.; Huang, C. G.** 2016. Progress in thermal-mechanical effects induced by laser, Advances in Mechanics 46: 201610 (in Chinese). https://doi.org/10.6052/1000-0992-15-025.
8. **Dimitrienko, Y. I.** 1999. Thermomechanics of Composites under High Temperatures. Springer Science & Business Media. https://doi.org/10.1007/978-94-015-9183-6.
9. **Lachaud, J.; Aspa, Y; Vignoles, G. L.** 2008. Analytical modeling of the steady state ablation of a 3D C/C composite, International Journal of Heat and Mass Transfer 51(9-10): 2614-2627. https://doi.org/10.1016/j.ijheatmasstransfer.2008.01.008.
10. **Zhang, J. F.** 2012. Experimental test and analysis for response of composite materials irradiated by laser. Beijing University of Technology (in Chinese).
11. **Zhao, W. N.; Huang, Y. H.; Song, H. W.; Huang, C. G.** 2017. Multi-scale analysis model of thermal-mechanical damage effect in high-power continuous-wave laser irradiation of CFRP laminates. Chinese journal of lasers 44(6): 0602003 (in Chinese). https://doi.org/10.3788/CJL201744.0602003.
12. **Zhu, K.; Long, L. C.** 2012. Numerical simulation and experiment contrast about laminated plate under laser irradiation, Chinese journal of lasers 39(1): 0103004 (in Chinese). https://doi.org/10.3788/CJL201239.0103004.
13. **Peng, G.L.; Du, T.J.; Liu, F.; Zhang, X. H.** 2014. Simulation study of laser energy coupling coefficient in the process of ablating glass fiber/epoxy composites, Chinese journal of lasers 41(2): 0203001 (in Chinese). https://doi.org/10.3788/CJL201441.0203001.
14. **Fu, D. S.; Qi, S. H.; Cheng, Y.; Li, Y.** 2010. Study on laser irradiation properties of T-700 carbon fiber reinforced plastic composite, Materials Reports 24(3): 39-41 (in Chinese).
15. **Li, G.** 2010. Numerical Research on the Macro-micro Effect of Laser Irradiation to Fibrous Composites. National University of Defense Technology (in Chinese).
16. **Wan, H.; Hu, K. W.; Mu, J. Y.; Bai, S. X.** 2008. Damage analysis of fiber reinforced resin matrix composites irradiated by CW laser. High power laser and particle beams 20(1): 6-10 (in Chinese).
17. **Xiong, L. J.; Wang, J. W.; Nie, G. H.** 2022. Analysis of ablation and strength of CFRP laminated structures under laser irradiation. Chinese quarterly of mechanics 43(4): 771-781 (in Chinese). https://doi.org/10.15959/j.cnki.0254-0053.2022.04.004.
18. **Han Y. C.; Wei C. H.; Zhang R.; Wang J.W.; Lv Y. W.** 2022. Experimental study on fracture behavior of preloaded CFRC laminate under laser irradiation, High Power Laser and Particle Beams 011011 (in Chinese). https://doi.org/10.11884/HPLPB202234.210329.
19. **Huang, Y. H.** 2015. Experimental and numerical simulation of multi-field coupling effect of a typical target irradiated by a strong laser. Doctoral Dissertation, Chinese Academy of Sciences University, Beijing (in Chinese).

20. **Xing, X. D.; Guo, W. L.; Duan, X.M.; Wang, L. Q.** 2019. Thermomechanical Coupling Damage and Analysis of Buckling Load of Laser Irradiated CFRP Cylinder Shell under Axial Load, Mechanika 25(2): 93-98. https://doi.org/10.5755/j01.mech.25.2.22340.
21. **Svante A.** 1889. Über die Reaktionsgeschwindigkeit bei der Inversion von Rohrzucker durch Säuren, Zeitschrift für Physikalische Chemie 4(1): 226–248. https://doi.org/10.1515/zpch-1889-0416.
22. **Lundell J.; Dickey R.** 1978. The response of heat-shield materials to intense laser radiation, Proceedings of the AIAA. 16th Aerospace Sciences Meeting. Huntsville, AL, USA. https://doi.org/10.2514/6.1978-138.

G. Yang, X. Xing, W. Guo, L. Wang

FINITE ELEMENT ANALYSIS OF LASER ABLATION DAMAGE AND BUCKLING MODE OF AXIALLY COMPRESSED CFRP CYLINDRICAL SHELL

S u m m a r y

Laser ablation damage has an important impact on the load-bearing capacity of the aircraft structure. This paper first uses ABAQUS ALE adaptive grid technology to establish and verify the numerical simulation analysis method of laser irradiation ablation of CFRP laminates. Then a finite element simulation analysis was conducted on the buckling process of the CFRP cylindrical shell under the combined loading conditions of laser irradiation and axial compression, and the critical buckling load and buckling mode of the cylindrical shell under different conditions were obtained. The effects of ablation damage and laser irradiation position on the critical buckling load are also discussed. When the laser irradiation position is between the end and the midpoint of the axis in the axial direction of the cylindrical, and is farthest from the axis in the radial direction, buckling failure is prone to occur.

Keywords: laser ablation, axial compression, CFRP cylindrical shell, thermo-mechanical coupling, critical buckling load.

Received December 6, 2023
Accepted June 20, 2024